RSC Advances

ROYAL SOCIETY OF CHEMISTRY

www.rsc.org/advances

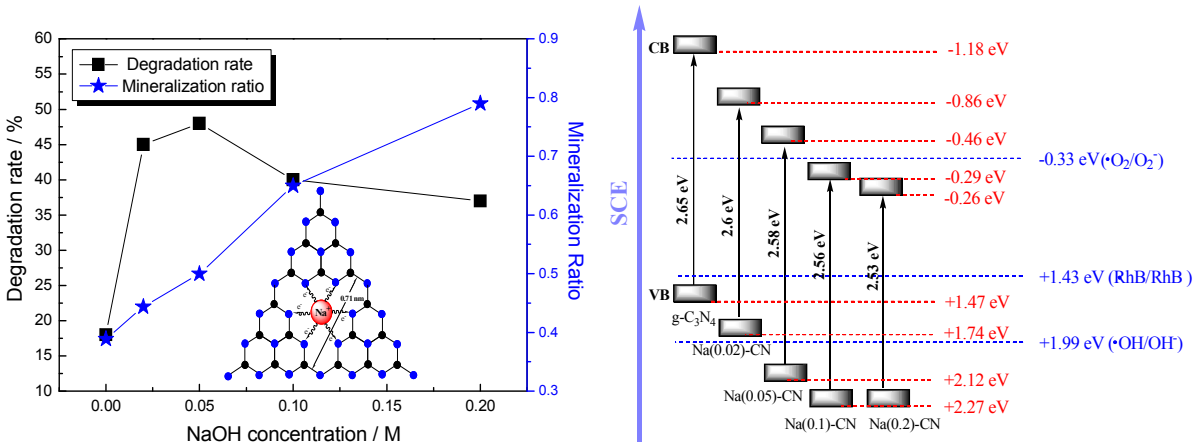

Sodium doped into g-C_3N_4 crystal lattice can tune the position of CB and VB potentials, influence the structural and optical properties and thus improve the Rhodamine B photodegradation and mineralization performances.

Cite this: DOI: 10.1039/c0xx00000x

www.rsc.org/xxxxxx

ARTICLE TYPE

A convenient method to prepare novel alkali metal sodium doped carbon nitride photocatalyst with a tunable band structure

Jian Zhang, [a] Shaozheng Hu [b,*] and Yanjuan Wang [a]

Received (in XXX, XXX) Xth XXXXXXXXX 20XX, Accepted Xth XXXXXXXXX 20XX

DOI: 10.1039/b000000x

A novel alkali metal sodium doped carbon nitride photocatalyst with a tunable band gap was prepared using dicyandiamide monomer and sodium hydrate as precursor. X-ray diffraction (XRD), N_2 adsorption, UV-Vis spectroscopy, Scanning electron microscopy (SEM), Photoluminescence (PL) and X-ray photoelectron spectroscopy (XPS) were used to characterize the prepared catalysts. The CB and VB potentials of graphitic carbon nitride could be tuned by controlling the sodium concentration. Besides, sodium doping inhibited the crystal growth of graphitic carbon nitride, enhanced the surface area and increased the separation rate of photogenerated electrons and holes. The visible-light-driven Rhodamine B (RhB) photodegradation and mineralization performances were significantly improved after sodium doping. The possible influence mechanism of sodium concentration on photocatalytic performance was proposed.

Introduction

Challenges of energy shortage and environmental pollution have raised awareness of a potential global crisis which human beings have to be faced. Among the various technologies to solve these problems, photocatalysis has attracted intensive interest for its promising applications because it can effectively utilize the abundant energy of either natural sunlight or artificial indoor illumination. Photocatalysis is widely used for hydrogen production as well as organic contaminants decomposition.[1] To use this technique, an efficient photocatalytic material is needed. The ideal photocatalytic material should possess a moderate band gap which absorbs light in the visible range and be efficient in separating, collecting and transporting charges for the chemical processes.[2] Besides, non-toxic, abundant and low-cost are also important for the ideal photocatalyst. Recently, graphitic carbon nitride ($g\text{-}C_3N_4$) has attracted much attention because of its potential to serve as photocatalyst,[3,4] electrode material for fuel cells,[5,6] catalyst for organic synthesis,[7,8] hydrogen storage material,[9] CO_2 capture material[10] etc. $g\text{-}C_3N_4$ is the most stable allotrope among the family of carbon nitrides. Also, $g\text{-}C_3N_4$ possesses high resistance to acids and alkalis, and is composed of very common elements, C, N and H only. As a photocatalyst, the $g\text{-}C_3N_4$ has a moderate band gap (2.7 eV), high chemical and thermal stability as well as fascinating electronic property. However, the rapid photogenerated electron-hole pair recombination leads to the low activity in practical applications.[11,12]

Development of $g\text{-}C_3N_4$ based heterostructured photocatalysts is one of the effective strategies to solve this problem. Heterojunctions are responsible for an efficient photogenerated charge interface migration, which is crucial for increasing the activity of photocatalysts. It is known that the energy level matching of two semiconductors is significantly important to form the heterojunction. A tunable band structure of $g\text{-}C_3N_4$ is convenient to match the energy level with other semiconductor, thus is beneficial for the forming of the heterojunction. In general, band gap of semiconductor nanocrystal can be controlled by the grain size, which called quantum size effect.[13] This size-dependent band gap of quantum dots has been extensively studied.[14] However, the preparation of quantum dots often requires harsh reaction conditions and complicated preparation procedure. Another facile and flexible approach is doping.[15-20] Orbital hybridization occurs between dopant orbital and molecular orbital of $g\text{-}C_3N_4$, leading to the tunable electronic structure and potential of VB and CB.

Because of the active chemical properties, alkali metal sodium is widely used in the catalytic reaction.[21-23] Jiang et al. reported the catalytic performance of X molecular sieve modified by Na^+ ions for the side-chain alkylation of toluene with methanol.[21] Yentekakis et al. investigated the comparative study of the $C_3H_6 + NO + O_2$, $C_3H_6 + O_2$ and $NO + O_2$ reactions in excess oxygen over Na-modified $Pt/g\text{-}Al_2O_3$ catalysts.[22] Chen et al. studied the formaldehyde oxidation on Pt/MnO_2 catalysts. They found that the Na^+ modification was demonstrated to be a facile and effective method to improve the catalysts performance for formaldehyde oxidation.[23] As for the influence of sodium on the photocatalytic performance, most of the investigations concern the effect of sodium ions on the morphology, structure and photocatalytic activity of nanotubular titanates.[24-26] Bern et al. found $Na^+ \rightarrow H^+$ replacement leads to a shortening titanate nanotube interlayer distance. Moreover, Na^+ concentration strongly influenced the optical property and band gap energy of prepared samples.[24] Qamar et al. considered that sodium ions

played a crucial role in the structural stability.[25] Turki et al. suggested that sodium mainly influences the structural transformation of titanate into anatase through a slow dehydration process.[26] As far as we know, no literature concerning the influence of sodium ions on the photocatalytic performance of g-C_3N_4 based catalyst was reported.

In addition to superior catalytic performance, the mineralization ability in the degradation process is a key issue impeded the practical application of photocatalysts. The photocatalytic degradation of organic compound is a complex process, and many intermediate products are produced, especially when the initial substrate is complicated. Many intermediate products are more harmful to human health than the initial pollutant. Thus thorough decomposition of the pollutant is necessary. In this work, a novel band gap-tunable sodium doped graphitic carbon nitride with enhanced mineralization ability was prepared for the first time using dicyandiamide monomer and sodium hydrate as precursor. The photocatalytic activity and stability were evaluated in the photocatalytic degradation of RhB under visible light. The effects of doping on the structural property, optical property and photocatalytic performance of as-prepared catalysts were discussed in detail.

Experimental

Preparation and characterization

In a typical experiment, 2 g dicyandiamide was dispersed into 10 ml deionized water under stirring. Then 10 ml NaOH solution (0.02, 0.05, 0.1 and 0.2 M) was added. The obtained suspension was heated to 100 ^oC to remove the water. The solid product was dried at 80 ^oC in oven, followed by milling and annealing at 520 ^oC for 2 h (at a rate of 5 $^oC \cdot min^{-1}$). The obtained product was denoted as Na(x)-CN, where x stands for the NaOH concentration. When 10 ml deionized water was used to replace NaOH following the same procedure as in the synthesis of Na(x)-CN, the product is denoted as g-C_3N_4. For comparison, as-prepared g-C_3N_4 was dispersed into 10 ml NaOH (0.05 M). The obtained suspension was stirred for 10 h, and heated to 100 ^oC to remove the water. The solid product was dried and denoted as NaOH/g-C_3N_4.

XRD patterns of the prepared samples were recorded on a Rigaku D/max-2400 instrument using Cu-Kα radiation (λ = 1.54 Å). The scan rate, step size, voltage and current was 0.05 ^{o}/min, 0.02, 40kV and 30 mA, respectively. UV-vis spectroscopy measurement was carried out on a JASCO V-550 model UV-vis spectrophotometer, using $BaSO_4$ as the reflectance sample. The morphology of prepared catalyst was observed by using a scanning electron microscope (SEM, JSM 5600LV, JEOL Ltd.). ICP was performed to determine the actual K concentration on a Perkin-Elmer Optima 3300DV apparatus. XPS measurements were conducted on a Thermo Escalab 250 XPS system with Al Kα radiation as the exciting source. The binding energies were calibrated by referencing the C 1s peak (284.6 eV) to reduce the sample charge effect. Curve fits were made using CasaXPS, while the relative sensitivity factors and asymmetry functions were taken from the PHI ESCA handbook. Nitrogen adsorption was measured at -196 °C on a Micromeritics 2010 analyzer. All the samples were outgassed at 393K for 3 h before the measurement. BET Surface area (S_{BET}) was calculated according to the adsorption isotherm. Photoluminescence (PL) spectra were measured at room temperature with a fluorospectrophotometer (FP-6300) using a Xe lamp as excitation source.

Photocatalytic Reaction

RhB was selected as the model compound to evaluate the photocatalytic performance of the prepared g-C_3N_4 based catalysts in an aqueous solution under visible light irradiation. 0.05 g catalyst was dispersed in 200 ml aqueous solution of RhB (10 ppm) in an ultrasound generator for 10 min. The suspension was transferred into a self-designed glass reactor, and stirred for 30 min in darkness to achieve the adsorption equilibrium. In the photoreaction under visible light irradiation, the suspension was exposed to a 250 W high-pressure sodium lamp with main emission in the range of 400-800 nm, and air was bubbled at 130 ml/min through the solution. The UV light portion of sodium lamp was filtered by 0.5 M $NaNO_2$ solution.[27] All runs were conducted at ambient pressure and 30 °C. At given time intervals, 4 ml suspension was taken and immediately centrifuged to separate the liquid samples from the solid catalyst. The concentrations of RhB before and after reaction were measured by UV-Vis spectrophotometer at a wavelength of 550 nm.

Results and discussion

Fig. 1 shows the XRD patterns of as-prepared g-C_3N_4, NaOH/g-C_3N_4 and Na(x)-CN. All the catalysts exhibit two peaks at 13.1^o and 27.3^o, corresponding to (100) and (002) crystal planes of g-C_3N_4 (JCPDS 87-1526).[3] For Na(x)-CN, the gradually decreased peak intensities are shown with increasing the sodium concentration. This suggests that the crystal growth of graphitic carbon nitride is inhibited by introduction of sodium. No peak for sodium related species is observed in the pattern of Na(x)-CN. Whereas, an obvious shift toward a lower 2θ value is observed for all the Na(x)-CN catalysts. This is probably due to that sodium doped into interstitial sites of in-planar g-C_3N_4 which enlarged the interlayer spacing. Compared with g-C_3N_4, no obvious peak shift and intensity decrease is observed in the pattern of NaOH/g-C_3N_4. This hints that the existence form of sodium species in NaOH/g-C_3N_4 and Na(0.05)-CN is different.

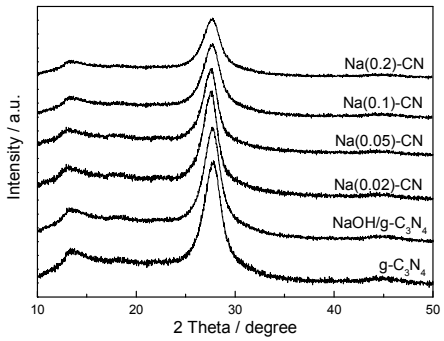

Fig. 1 XRD patterns of as-prepared g-C_3N_4, NaOH/g-C_3N_4 and Na(x)-CN.

Nitrogen adsorption and desorption isotherms were measured

to characterize the specific surface area of as-prepared g-C_3N_4 based catalysts (Fig. 2). The isotherm of both g-C_3N_4 and Na(0.05)-CN are of classical type IV, suggesting the presence of mesopores. The hysteresis loop in the low pressure range ($0.4<P/P_0<0.9$) is associated with the intra-aggregated pores. The high-pressure hysteresis loop ($0.9<P/P_0<1$) is related to the larger pores formed between secondary particles. The BET specific surface areas (S_{BET}) of g-C_3N_4, Na(0.02)-CN, Na(0.05)-CN, Na(0.1)-CN, Na(0.2)-CN and NaOH/g-C_3N_4 are calculated to be 8.9, 20.8, 29.6, 33.5, 37.3 and 9.5 $m^2 \cdot g^{-1}$, respectively. This increased S_{BET} is probably due to that sodium doping inhibits the crystal growth of graphitic carbon nitride, leading to the formation of more secondary particles. Such large S_{BET} is favorable to the photocatalytic performance because it can promote adsorption, desorption and diffusion of reactants and products.

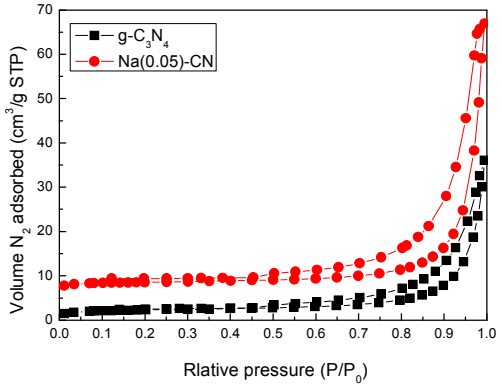

Fig. 2 N_2 adsorption-desorption isotherm of g-C_3N_4 and Na(0.05)-CN.

The morphologies of representative catalysts were examined by using SEM. Fig. 3a shows that as-prepared g-C_3N_4 composes of a large number of irregular particles. Those particles exhibit layered structure, similar to its analogue graphite (Fig. 3a, b). The size of layered structure of Na(0.05)-CN is obviously decreased compared with g-C_3N_4. This indicates that sodium doping could inhibit crystal growth of graphitic carbon nitride which is consistent with the XRD result. The elemental mapping image shown in Fig. 3c indicates that sodium is homogenously distributed in the whole host of g-C_3N_4.

Fig. 4 shows the UV-Vis diffuse reflectance spectra of as-prepared g-C_3N_4 based catalysts. The g-C_3N_4 shows typical semiconductor absorption, originating from charge transfer response of g-C_3N_4 from the VB populated by N 2p orbitals to the CB formed by C 2p orbitals.[3] The band gap energy of g-C_3N_4 estimated with the Kubelka-Munk function is about 2.65 eV, which is in good agreement with the value reported in previous literature.[28] Compared with g-C_3N_4, the obvious red shifts of the absorption band are observed in the spectra of Na(x)-CN but not in that of NaOH/g-C_3N_4. This confirms that the existence form of sodium species in NaOH/g-C_3N_4 and Na(x)-CN is different. The inset in Fig. 4 reveals that pure g-C_3N_4 is light yellow in colour. The color of Na(x)-CN gradually deepens with increasing the sodium concentration. The band gap energy decreases to 2.58, 2.56 and 2.53 eV for Na(0.02)-CN, Na(0.05)-CN, Na(0.1)-CN and Na(0.2)-CN, respectively. This indicates that sodium concentration strongly influenced the optical property and band structure of as-prepared g-C_3N_4 based catalysts. Ma et al. calculated the electronic structure of phosphorus doped g-C_3N_4 using first-principles.[29] They found that isolated P 3p orbital was localized below the bottom of the CB in the host g-C_3N_4, thus decreased the band gap energy. Similarly, after sodium doping, an isolated atomic orbitals of dopant may locate in the g-C_3N_4 band gap, or orbital hybridization occurs between dopant orbitals and molecular orbitals of g-C_3N_4, leading to the altered potential of VB and CB.

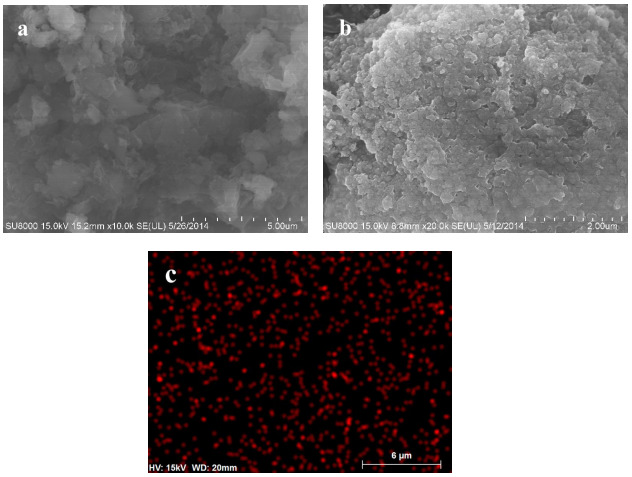

Fig. 3 SEM images of g-C_3N_4 (a), Na(0.05)-CN (b) and elemental mapping image of Na (c).

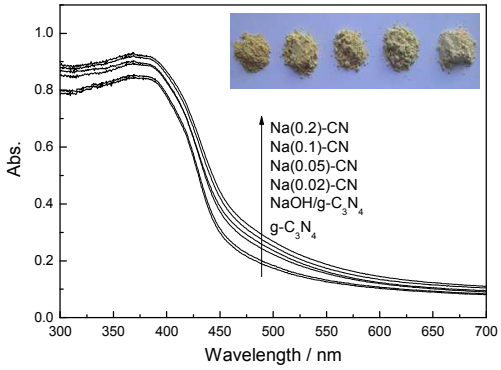

Fig. 4 UV-Vis diffuse reflectance spectra of as-prepared g-C_3N_4 based catalysts.

In order to confirm the structure of prepared catalysts and to further identify the chemical status of Na element, as-prepared catalysts were characterized by XP spectra. In Fig. 5a and b, the spectra of g-C_3N_4 in both N 1s and C 1s regions can be fitted with two contributions. In Fig. 5a, the main N 1s peak at a binding energy of 398.5 eV can be assigned to sp^2 hybridized nitrogen (C=N–C), thus confirming the presence of sp^2 bonded graphitic carbon nitride. The peak at higher binding energy 400.5 eV is attributed to tertiary nitrogen (N–$(C)_3$) groups.[30] In C 1s region

(Fig. 5b), two components locate at 284.6 and 287.8 eV for g-C_3N_4. The sharp peak around 284.6 eV is attributed to the pure graphitic species in the CN matrix. The peak with binding energy of 287.8 eV indicates the presence of sp^2 C atoms bonded to aliphatic amine (–NH_2 or –NH–) in the aromatic rings.[31,32] In the case of Na(0.05)-CN, a slight shift to lower binding energy is observed in N 1s but not in C 1s region compared with that of g-C_3N_4. This is probably due to the higher electronegativity of N atoms, leading to the formation of strong interaction with doped sodium. The electrons of sodium could be transferred to nitrogen, causing the increased electron density of N atoms.

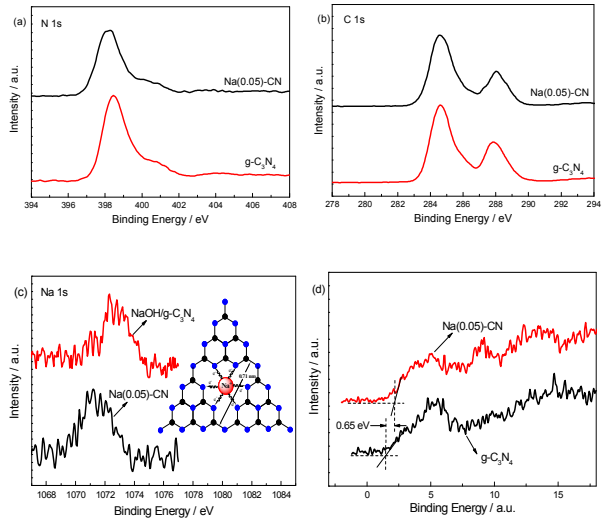

Fig. 5 XP spectra of as-prepared catalysts in the region of N 1s (a), C 1s (b), Na 1s (c) and VB XPS (d).

Fig. 5c shows that the binding energy of NaOH/g-C_3N_4 in Na 1s region is located at 1072.6 eV, which should be attributed to the Na-O group in Na_2O.[33] In the case of Na(0.05)-CN, the binding energy is 1071.3 eV, obviously lower than that of NaOH/g-C_3N_4. The Na concentration obtained by ICP is 0.52, 1.06, 1.98, 3.85 and 1.02 wt.% in Na(0.02)-CN, Na(0.05)-CN, Na(0.1)-CN, Na(0.2)-CN and NaOH/g-C_3N_4 respectively. Besides, the calculation result of surface elemental concentration determined by XPS reveals that Na concentration in Na(0.05)-CN is 1.14 wt.%, which is close to the ICP result (1.06 wt.%). In the case of NaOH/g-C_3N_4, this value is 3.72 wt.%, much higher than that of ICP result (1.02 wt.%). This is probably due to the different existence form of Na species in two samples. For NaOH/g-C_3N_4, Na species mainly exists on the surface. Whereas Na could be doped into g-C_3N_4 lattice during the polycondensation process, leading to the uniform dispersion in the bulk of Na(0.05)-CN. Moreover, because the electronegativity of N atoms is lower than the O atoms, the electron density of sodium in Na-N bond should be higher than that in Na-O group, leading to the binding energy difference (Fig. 5c). Besides, the binding energy of Na(0.05)-CN in Na 2s region is located at 62.7 eV, which is in good agreement with the reported binding energy of Na 2s for NaN_3 (not shown here).[34] This confirms that the Na ions are coordinated into the big C-N rings formed by N-bridge linking the triazine units in the plane of g-C_3N_4. It is known that the lone pair electron of nitrogen plays an important role in the electron density distribution, strongly influences the electronic structure of carbon nitride.[35] Na doping could influence the electron density of N atoms, thus alter the electronic structure and band gap of carbon nitride. As for the doping site of Na, the probably situation is interstitial sites. It is known that g-C_3N_4 is covalent compound. Na could not be doped as ion state in substitutional site. Moreover, the atomic radius of C and N (70 and 65 pm) is much smaller than that of Na^+ (~100 pm). Elemental analyse results reveals that the C/N ratios for Na(0.05)-CN, Na(0.1)-CN and Na(0.2)-CN are 0.70, 0.71 and 0.70, very similar to that of g-C_3N_4 (0.71). This confirms that interstitial doping but not substitutional doping occurred. The maximum in-planar distance of nitride pores is 0.71 nm,[29] which is adequate to accommodate the Na^+ ions. In addition, it is well known that the C-O ring in 18-crown-6 exhibits the strong capability to capture metal cations such as Na^+ by forming an ion-dipole interaction between the cations and the negatively charged oxygen of the polyether ring.[36] Compared to the oxygen atoms in the C-O ring of 18-crown-6, the nitrogen atoms of the nitrogen pots of g-C_3N_4 are also ideal sites for metal ion inclusion with stronger coordination ability due to more lone-pair electrons. Summarizing the above results, the possible doping site of Na^+ ions in Na(x)-CN is shown in Fig. 5c.

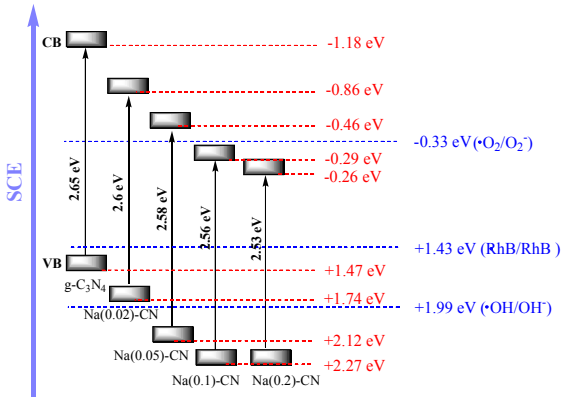

Fig. 6 Band gap structures of as-prepared g-C_3N_4 and Na(x)-CN.

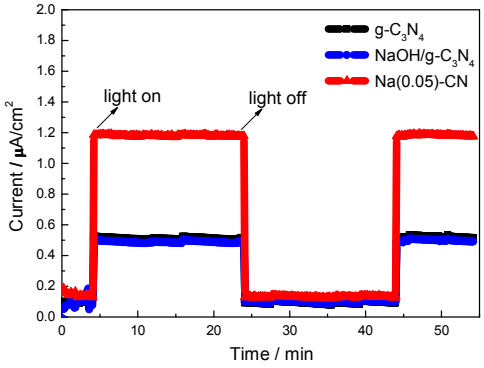

Fig. 7 The photocurrent responses of g-C_3N_4, NaOH/g-C_3N_4 and Na(0.05)-CN.

To further investigation the influence of Na doping on the relative positions of CB and VB, the VB XP spectra was employed to determine the electronic structure (Fig. 5d). Compared with the spectrum of g-C_3N_4, an obvious shift (0.65 eV) is shown in Na(0.05)-CN, which should be attributed to the Na atoms doped into g-C_3N_4 lattice. The VB of g-C_3N_4 and Na(0.05)-CN locate at +1.47 and +2.12 eV. Combined with the UV-Vis result, the optical CB potentials of g-C_3N_4 and Na(0.05)-CN locate at -1.18 and -0.46 eV. The VB and CB potentials of other Na doped g-C_3N_4 catalysts are calculated and shown in Fig. 6. Obviously, the CB and VB positions are gradually altered with increasing the Na concentration. The CB and VB potentials could be tuned from -1.18 and +1.47 eV to -0.26 and +2.27 eV by controlling the Na concentration. Such tunable CB and VB potentials are beneficial to the forming of the heterojunction with other semiconductors in order to meet different application demands.

The outstanding carrier separation ability is confirmed by the photocurrent responses measurement (I-t curve, Fig. 7). Without doubt, compared with g-C_3N_4, no obvious photocurrent improvement is observed for NaOH/g-C_3N_4. The photocurrent value of Na(0.05)-CN is ~2.4 times as high as that of g-C_3N_4, which can be attributed to the improved interfacial charge transfer ability. Besides, the photocurrent responses do not decay with the increased illuminated time, indicating the prepared catalysts could provide stable quantity of electrons and holes during the irradiation. This hints that the prepared catalysts should exhibit the stable photocatalytic activities.

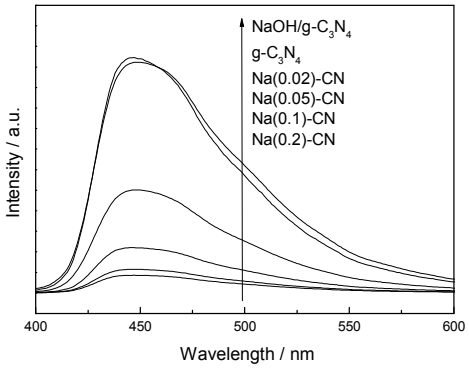

Fig. 8 PL spectra of as-prepared g-C_3N_4 based catalysts.

It is known that a certain amount of chemical energy is released during the recombination process of photoinduced charge carriers. Such chemical energy is further transformed to light energy, which is dissipated as radiation. This results in a luminescence emission, called the PL phenomenon. PL is a highly sensitive technique used to investigate the photophysical and photochemical properties of solid semiconductors, and can provide information on charge separation/recombination of photoinduced charged carriers (electron/hole), as well as surface defects.[37] In general, the lower PL intensity, the higher separation rates of photogenerated e^-/h^+ pairs. Fig. 8 shows the room temperature PL spectra of as-prepared g-C_3N_4 based catalysts under the excitation wavelength of 380 nm. For g-C_3N_4, the broad PL band is around 465 nm, which is attributed to the band-band PL phenomenon with the energy of light approximately equal to the band gap of g-C_3N_4.[31] No essential difference in PL curves between g-C_3N_4 and NaOH/g-C_3N_4 is observed, indicating this modification method do not improve the separation rate of photogenerated electrons-holes pairs. In the case of Na(x)-CN, the shape of the curves are similar to that of g-C_3N_4, whereas the peak intensities decrease sharply. This is probably due to that Na doping gives rise to distortion in the lattice structure of g-C_3N_4, causes the increased surface energy, enhances the interfacial charge transfer rate, thus leading to the reduced recombination rate of electron-hole pair. Such increased separation rate of photogenerated electrons-holes pairs in Na(x)-CN catalysts could improve the visible light utilization, thus is beneficial to the photocatalytic performance.

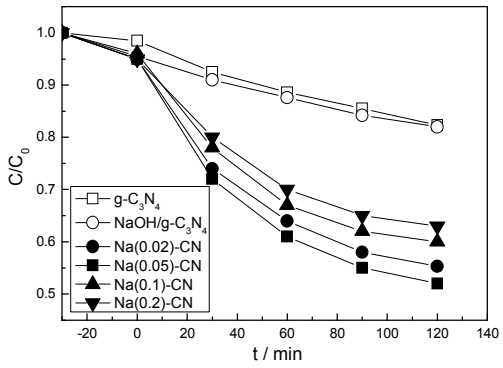

Fig. 9 Photocatalytic performances of as-prepared g-C_3N_4 based catalysts in the degradation of RhB under visible light irradiation.

Fig. 9 shows the photocatalytic performances of as-prepared g-C_3N_4 based catalysts in the degradation of RhB under visible light irradiation. Before the light on, the RhB adsorption abilities of Na(x)-CN catalysts are improved, which is probably due to the larger S_{BET}. Control experiment results indicate that the RhB degradation performance can be ignored in the absence of either irradiation or photocatalyst, indicating that RhB is degraded via photocatalytic process. Without doubt, NaOH/g-C_3N_4 exhibits almost the same photocatalytic activity as g-C_3N_4. Whereas Na(x)-CN catalysts show clearly improved photocatalytic performance. This is probably due to the synergistic effect caused by the Na doping which improved the S_{BET}, decreased the band gap energy and enhanced the separation rate of photogenerated electrons-holes pairs. The photocatalytic activity enhances with increasing the Na concentration from 0.02 to 0.05. Na(0.05)-CN showed much higher photocatalytic activity than that of other Na doped catalysts. When Na concentration beyond 0.05, the activity decreases remarkably. The possible reason is discussed (see below).

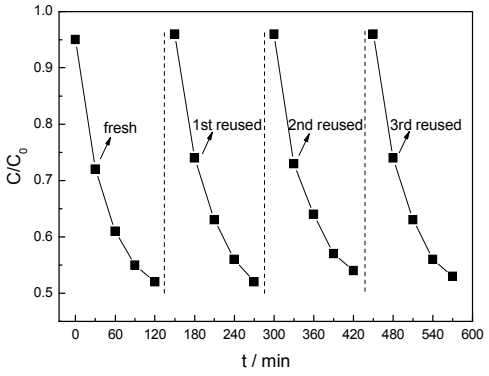

Fig. 10 Photocatalytic stability of Na(0.05)-CN.

The reaction rate constant k was obtained by assuming that the reaction followed first order kinetics.[38] In a batch reactor, the performance equation is as follows: $-\ln(C/C_0) = kt$ where C_0 and C represent the concentrations of RhB dye before and after photocatalytic degradation, respectively. If a linear relationship is established when $-\ln(C/C_0)$ is plotted against t (reaction time), the rate constant k can be obtained from the slope of the line. The calculated results indicate that the rate constant k are 0.0018, 0.0058, 0.0064, 0.0047 and 0.0041 min^{-1} for g-C_3N_4, Na(0.02)-CN, Na(0.05)-CN, Na(0.1)-CN and Na(0.2)-CN, respectively. Na(0.05)-CN shows the highest rate constant, which is 3.5 times higher than that of g-C_3N_4. The catalytic stability test of as-prepared Na(0.05)-CN was carried out (Fig. 10). The results indicate that no obvious decrease in RhB degradation performance is observed after three cycles. ICP result displays that the Na concentration is 1.03 wt.% in reused Na(0.05)-CN which is very close to the fresh catalyst (1.06 wt.%). Therefore, it is deduced that the as-prepared Na(0.05)-CN is stable. However, the ICP result indicates that the Na concentration of used NaOH/g-C_3N_4 decreases sharply to 0.32 wt.%, probably due to that Na^+ dissolved into the solution. To confirm this point of view, the pH values of Na(0.05)-CN and NaOH/g-C_3N_4 suspension were measured by pH meter. The results show that the suspension of Na(0.05)-CN is almost neutral (pH=7.22). For NaOH/g-C_3N_4, the pH value is 9.68, much higher than that of Na(0.05)-CN.

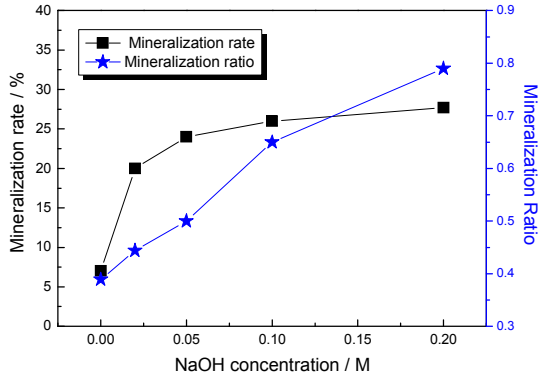

Fig. 11 Mineralization rate and mineralization ratio comparison of as-prepared g-C_3N_4 based catalysts.

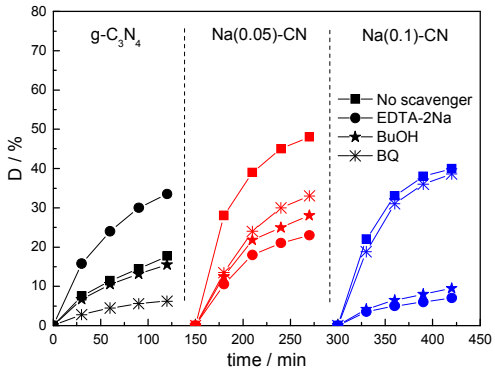

Fig. 12 Influence of various scavengers on the visible light photocatalytic activity of g-C_3N_4, Na(0.05)-CN and Na(0.1)-CN.

The mineralization ability of prepared catalysts to RhB molecules was evaluated by monitoring the changes of TOC in the reaction systems. Fig. 11 shows the mineralization rate and mineralization ratio comparison of as-prepared g-C_3N_4 based catalysts. Mineralization ratio, which represents the mineralization ability is equal to the ratio of the mineralization rate to the degradation rate. Obviously, the mineralization ratios increase evidently with increasing NaOH concentration. Zhang et al. prepared TCNQ-g-C_3N_4 organic composite photocatalysts for phenol degradation. They suggested that the enhancement of mineralization ability was attributed to the lower valence position which caused by the formation of conjugative π structure material hybridized photocatalysts.[39] In this investigation, Na doping can alter the band structure of as-prepared g-C_3N_4 based catalysts, thus improve the mineralization ability.

The hole and free radical trapping experiments were carried out to clarify the reaction mechanism and the active species generated during the reaction process. In this investigation, EDTA-2Na, tert-butyl alcohol (t-BuOH) and 1,4-benzoquinone (BQ) are used as the hole (h^+), hydroxyl radical (•OH) and superoxide radical ($•O_2^-$) scavenger, respectively. Fig. 12 shows the influence of various scavengers on the visible light photocatalytic activity of g-C_3N_4, Na(0.05)-CN and Na(0.1)-CN. For g-C_3N_4, the photodegradation rate of RhB only decreases slightly after the addition of t-BuOH, but sharply when BQ is added. This indicates that the main active species is not hydroxyl radicals but $•O_2^-$ in the current photocatalytic systems. In theory, the CB and VB position of g-C_3N_4 are -1.12 V and +1.57 V, respectively.[40] The redox potentials of $•OH/OH^-$ and $O_2/•O_2^-$ are +1.99 V and -0.33 V, as shown in Fig. 6.[41] Obviously, the reduction potential of CB electrons in g-C_3N_4 is more negative than the redox potential of $O_2/•O_2^-$ which can reduce O_2 to form $•O_2^-$, whereas the VB holes in g-C_3N_4 are not positive enough to generate •OH. This theoretical result is consistent with our experiment results. In the presence of EDTA-2Na, the degradation rate is increased obviously, which is completely different from previous results.[39] Zhang et al. prepared $C_3N_4/Bi_5Nb_3O_{15}$ heterojunction catalyst for 4-CP photodegradation.[39] The photodegradation rate decreased significantly after the addition of EDTA-2Na, indicating the photogenerated holes were the main active species in their

system. In this study, although the redox potential of RhB is reported to be 1.43 V,[42] which is higher than the VB of g-C_3N_4 (Fig. 7), the direct photogenerated holes oxidation do not occur. On the contrary, the addition of EDTA-2Na to trap the h^+ could promote the separation rate of electron-hole pairs, leading to the increased photocatalytic performance. In the case of Na(0.05)-CN, the activity decreases obviously when each scavenger is added, suggesting both •OH and $•O_2^-$ are the main active species in this photocatalytic system. This is due to the change of VB and CB positions after Na doping. The VB potential is +2.12 eV, more positive than the redox potential of $•OH/OH^-$. Therefore, OH^- could trap the h^+ to form •OH, which is responsible for RhB degradation. For Na(0.1)-CN, the VB and CB potentials are +2.27 and -0.29 eV, as shown in Fig. 6. The CB potential decreases obviously, even lower than that of redox potential of $O_2/•O_2^-$. Therefore, when BQ is added, only slight decrease in activity is observed. Moreover, the addition of EDTA-2Na and BuOH remarkably decreases the activity confirms that the main active species is •OH in this photocatalytic system. Because the positions of VB and CB of Na(x)-CN are obviously altered by controlling the Na concentration, both •OH and $•O_2^-$ could be formed in Na(0.05)-CN system. Therefore, it is reasonable that Na(0.05)-CN shows much higher activity than that of other sodium doped catalysts.

Conclusions

A novel alkali metal sodium doped carbon nitride photocatalyst with a tunable band structure was prepared using dicyandiamide monomer and sodium hydrate as precursor. Sodium doped g-C_3N_4 exhibited smaller grain size, larger S_{BET}, narrower band gap energy and better separation rate of photogenerated electrons and holes. The CB and VB potentials of as-prepared Na(x)-CN could be tuned by controlling the Na concentration. The RhB photodegradation and mineralization performances were significantly improved after sodium doping under visible light. Because of the regulating effect of sodium doping on band structure, both •OH and $•O_2^-$ could be formed in Na(0.05)-CN reaction system, leading to its activity much higher than that of other sodium doped catalysts. Na(0.05)-CN showed the highest rate constant, which was 3.5 times higher than that of g-C_3N_4. Moreover, Na(0.05)-CN exhibited stable catalytic activity and chemical structure.

Acknowledgment

The authors are grateful for financial support from the National Natural Science Foundation of China (No. 21276253, 21103077), Education Department of Liaoning Province (No. L2013150) and the Natural Science Foundation of Liaoning Shihua University (No. 2011XJJ-021).

Notes and references

[a] *School of Petrochemical Engineering, Liaoning Shihua University, Fushun 113001, PR China.*
[b] *Institute of Eco-environmental Sciences, Liaoning Shihua University, Fushun 113001, PR China. E-mail: hushaozhenglnpu@163.com; Tel: 86-24-56860865*

1 M.R. Hoffmann, S.T. Martin, W. Choi and D.W. Bahnemann, *Chem. Rev.,* 1995, **95**, 69.
2 H. Kisch, *Angew. Chem. Int. Ed.,* 2013, **52**, 812.
3 Y. Wang, X.C. Wang and M. Antonietti, *Angew. Chem. Int. Ed.,* 2012, **51**, 68.
4 P.D. Tran, L.H. Wong, J. Barber and J.S.C. Loo, *Energy Environ. Sci.,* 2012, **5**, 5902.
5 Y. Zheng, J. Liu, J. Liang, M. Jaroniec and S.Z. Qiao, *Energy Environ. Sci.,* 2012, **5**, 6717.
6 Y. Zheng, Y. Jiao, M. Jaroniec, Y. Jin and S.Z. Qiao, *Small,* 2012, **8**, 3550.
7 X.F. Chen, J.S. Zhang, X.Z. Fu, M. Antonietti and X.C. Wang, *J. Am. Chem. Soc.,* 2009, **131**, 11658.
8 M.B. Ansari, H.L. Jin, M.N. Parvin and S.E. Park, *Catal. Today,* 2012, **185**, 211.
9 G. Koh, Y.W. Zhang and H. Pan, *Int. J. Hydrogen Energy,* 2012, **37**, 4170.
10 Q.F. Deng, L. Liu, X.Z. Lin, G.H. Du, Y.P. Liu and Z.Y. Yuan, *Chem. Eng. J.,* 2012, **203**, 63.
11 K. Sridharan, E. Jang and T.J. Park, *Appl. Catal. B: Environ.,* 2013, **142-143**, 718.
12 P. Niu, L. Zhang, G. Liu and H. Cheng, *Adv. Funct. Mater.,* 2012, **22**, 4763.
13 D.C. Pan, D. Weng, X.L. Wang, Q.F. Xiao, W. Chen, C.L. Xu, Z.Z. Yang and Y.F. Lu, *Chem. Commun.,* 2009, 4221.
14 A.P. Alivisatos, *Science,* 1996, **271**, 933.
15 S.C. Yan, Z.S. Li and Z.G. Zou, *Langmuir,* 2010, **26**, 3894.
16 G. Liu, P. Niu, C.H. Sun, S.C. Smith, Z.G. Chen, G.Q. Lu and H.M. Cheng, *J. Am. Chem. Soc.,* 2010, **132**, 11642.
17 Y.J. Zhang, T. Mori, J.H. Ye and M. Antonietti, *J. Am. Chem. Soc.,* 2010, **132**, 6294.
18 L.G. Zhang, X.F. Chen, J. Guan, Y.J. Jiang, T.G. Hou and X.D. Mu, *Mater. Res. Bull.,* 2013, **48**, 3485.
19 G.G. Zhang, M.W. Zhang, X.X. Ye, X.Q. Qiu, S. Lin and X.C. Wang, *Adv. Mater.,* 2014, **26**, 805.
20 S.Z. Hu, L. Ma, J.G. You, F.Y. Li, Z.P. Fan, G. Lu, D. Liu and J.Z. Gui, *Appl. Surf. Sci.,* 2014, **311**, 164.
21 J. Jiang, G.Z. Lu, C.X. Miao, X. Wu, W.H. Wu and Q. Sun, *Micro. Meso. Mater.,* 2013, **167**, 213.
22 I.V. Yentekakis, V. Tellou, G. Botzolaki and I.A. Rapakousios, *Appl. Catal. B: Environ.,* 2005, **56**, 229.
23 Y. Chen, J.H. He, H. Tian, D.H. Wang and Q.W. Yang, *J. Colloid Inter. Sci.,* 2014, **428**, 1.
24 V. Bem, M.C. Neves, M.R. Nunes, A.J. Silvestre and O.C. Monteiro, *J. Photochem. Photobio. A: Chem.,* 2012, **232**, 50.
25 M. Qamar, C.R. Yoon, H.J. Oh, N.H. Lee, K. Park, D.H. Kim, K.S. Lee, W.J. Lee and S.J. Kim, *Catal. Today,* 2008, **131**, 3.
26 A. Turki, H. Kochkar, C. Guillard, G. Berhault and A. Ghorbel, *Appl. Catal. B: Environ.,* 2013, **138-139**, 401.
27 F.B. Li, X.Z. Li, M.F. Hou, K.W. Cheah and W.C.H. Choy, *Appl. Catal. A,* 2005, **285**, 181.
28 G.Q. Li, N. Yang, W.L. Wang and W.F. Zhang, *J. Phys. Chem. C,* 2009, **113**, 14829.
29 X.G. Ma, Y.H. Lv, J. Xu, Y.F. Liu, R.Q. Zhang and Y.F. Zhu, *J. Phys. Chem. C,* 2012, **116**, 23485.
30 Y.W. Zhang, J.H. Liu, G. Wu and W. Chen, *Nanoscale,* 2012, **4**, 5300.
31 L. Ge and C. Han, *Appl. Catal. B: Environ.,* 2012, **117-118**, 268.
32 W. Lei, D. Portehault, R. Dimova and M. Antoniettit, *J. Am. Chem. Soc.,* 2011, **133**, 7121.
33 M. Ruckh, D. Schmid, M. Kaiser, R. Schaffler, T. Walter and H. Schock, *Sol. Energy Mater. Sol. Cells,* 1996, **41-42**, 335.
34 H.L. Gao, S.C. Yan, J.J. Wang, Y.A. Huang, P. Wang, Z.S. Lia and Z.G. Zou, *Phys. Chem. Chem. Phys.,* 2013, **15**, 18077.
35 G.P. Dong, Y.H. Zhang, Q.W. Pan and J.R. Qiu, *J. Photochem. Photobiol. C: Photochem. Rev.,* 2014, **20**, 33.
36 C.J. Pedersen, *J. Am. Chem. Soc.,* 1967, **89**, 7017.
37 J.Y. Shi, J. Chen, Z.C. Feng, T. Chen, Y.X. Lian, X.L. Wang and C. Li, *J. Phys. Chem. C,* 2007, **111**, 693.
38 X.Y. Li, D.S. Wang, G.X. Cheng, Q.Z. Luo, J. An and Y.H. Wang, *Appl. Catal. B: Environ.,* 2008, **81**, 267.

39 M. Zhang, W.Q. Yao, Y.H. Lv, X.J. Bai, Y.F. Liu, W.J. Jiang, Y.F. Zhu, *J. Mater. Chem. A,* 2014, **2**, 11432.
40 X.C. Wang, K. Maeda, A. Thomas, K. Takanabe, G. Xin, K. Domen and M. Antonietti, *Nat. Mater.,* 2009, **8**, 76.
41 G. Liu, P. Niu, L.C. Yin and H.M. Cheng, *J. Am. Chem. Soc.,* 2012, **134**, 9070.
42 T. Shen, Z.G. Zhao, Q. Yu and H.J. Xu, *J. Photochem. Photobiol. A: Chem.,* 1989, **47**, 203.